

## Electronic Supplementary Material

# **Construction of multi-hollow polymer microspheres with tailored mesoporous wall**

Hanqin Weng,<sup>a,b</sup> Zhihao Wu,<sup>a</sup> Chi Zhao,<sup>b,c</sup> Mozhen Wang,<sup>\*b</sup> Xuewu Ge,<sup>b</sup> Shinichi Yamashita,<sup>d,e</sup> Jia Tang,<sup>a</sup> and Mingzhang Lin<sup>a,f</sup>

<sup>a</sup> *Department of Engineering and Applied Physics, School of Physical Sciences, University of Science and Technology of China, Hefei, Anhui, 230026, China*

<sup>b</sup> *CAS Key Laboratory of Soft Matter Chemistry, Department of Polymer Science and Engineering, University of Science and Technology of China, Hefei, Anhui, 230026, China*

<sup>c</sup> *Wanhua Chemical Group Co., Ltd., Yantai, Shandong, 264006, China*

<sup>d</sup> *Nuclear Professional School, School of Engineering, The University of Tokyo, 2-22 Shirakata-shirane, Tokai-mura, Naka-gun, Ibaraki 319-1188, Japan*

<sup>e</sup> *Department of Nuclear Engineering and Management, School of Engineering, The University of Tokyo, 4-7-1 Hongo, Bunkyo-ku, Tokyo 113-8656, Japan*

<sup>f</sup> *Institute of Nuclear Energy Safety Technology, Chinese Academy of Sciences, Hefei, Anhui, 230031, China*

\* To whom the correspondence should be addressed. E-mail: pstwmz@ustc.edu.cn;

Tel: +86-0551-63600843

## I. Synthesis of Macro@Meso-SPS microspheres

The TEM images of PS and SPS microspheres were obtained on transmission electron microscope (H-7650) at an accelerate voltage of 100 kV. The Samples were prepared by dropping the ethanol dispersion of microspheres onto a piece of copper grids and being dried at ambient temperature. The weight average diameter ( $D_w$ ), number average diameter ( $D_n$ ), and polydispersion index of the diameters ( $PDI_D$ ) were calculated by the following equations. At least 100 microspheres were measured in the TEM images.

$$D_w = \frac{\sum n_i D_i^4}{\sum n_i D_i^3}, \quad D_n = \frac{\sum n_i D_i}{\sum n_i}, \quad PDI_D = \frac{D_w}{D_n}$$

where  $n_i$  is the number of particles with a diameter of  $D_i$ . The  $D_n$  and PDI are listed in the Table S1.

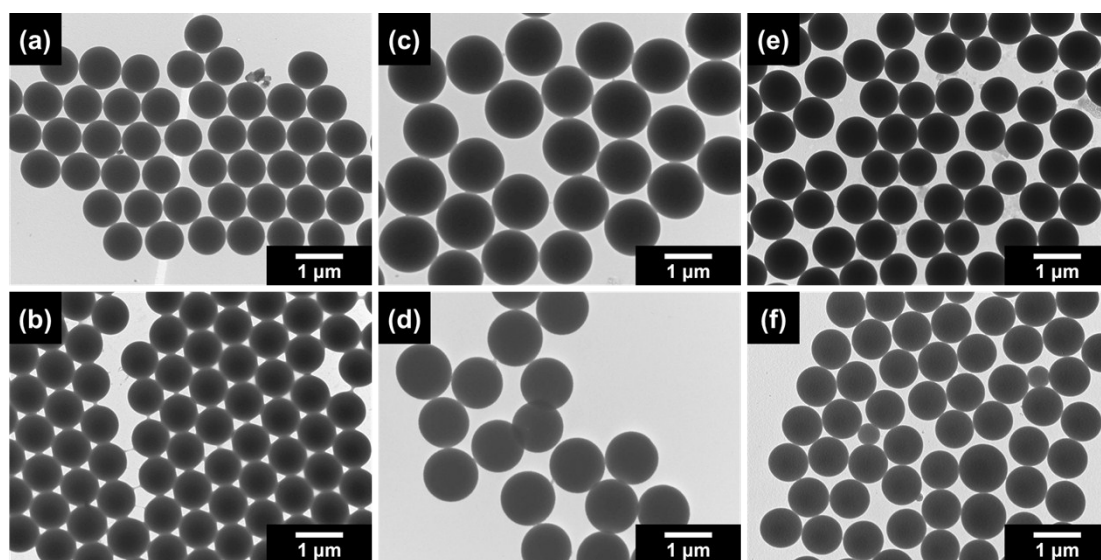


**Fig. S1.** TEM images of PS-R1 (a), SPS-R1 (b), PS-R2 (c), SPS-R2 (d), PS-C (e), and SPS-C (f) microspheres

Table S1 The synthetic condition and the size of different original PS microspheres

	St (mL)	PVP (g)	Solvent		AIBN (mg)	$\dot{D}$ (Gy min <sup>-1</sup> )	$D$ (kGy)	$D_n$ ( $\mu\text{m}$ )	PDI <sub>D</sub>
			ethanol (mL)	water (mL)					
PS-R1	4	1	15	1	0	60	54	0.81	1.004
PS-R2	4	1	15	1	0	80	72	1.15	1.004
PS-C	10	1	95	5	80	-	-	0.83	1.010

Table S2 The degree of sulfonation and the size of different SPS seed microspheres

	original PS microspheres	$DS_{XPS}$ (%) <sup>§</sup>	$DS_{EA}$ (%) <sup>§</sup>	$D_n$ (μm)	$PDI_D$
SPS-R1	PS-R1	45.45	2.04	1.14	1.004
SPS-C	PS-C	54.80	2.33	0.84	1.020

<sup>§</sup> The degree of sulfonation ( $DS$ ) of the SPS microspheres measured from XPS ( $DS_{XPS}$ ) and EA ( $DS_{EA}$ ) analysis was obtained according to the following Eqs S1 and S2, respectively:

$$DS_{XPS} = 8 \left( \frac{\text{atom\% S}}{\text{atom\% C}} \right) \times 100\% \quad (\text{S1})$$

$$DS_{EA} = \left( \frac{96}{32} \right) \left( \frac{\text{wt\% S}}{\text{wt\% C}} \right) \times 100\% \quad (\text{S2})$$

$DS_{EA}$  can be considered as the  $DS$  of the whole SPS microspheres, while  $DS_{XPS}$  is the  $DS$  of the surface layer of SPS microspheres since the detection depth of XPS is only about 5 nm. The data of SPS microspheres measured by XPS and EA were listed in Table S3 and Table S4, respectively.

Table S3 The XPS data of different SPS microspheres

	C ratio (at.%)	O ratio (at.%)	N ratio (at.%)	S ratio (at.%)
SPS-R1	77.62	15.25	2.71	4.41
SPS-C	74.60	17.26	3.03	5.11

Table S4 The EA data of different SPS microspheres.

	C ratio (wt.%)	H ratio (wt.%)	O ratio (wt.%)	N ratio (wt.%)	S ratio (wt.%)
SPS-R1	86.40	7.62	1.49	0.23	1.31
SPS-C	87.48	8.13	1.39	0.30	0.68

Table S5 The identifications (IDs) of the samples obtained after the SPS seed microspheres were treated in the swelling-osmosis and the PIPS processes with different conditions

Seed microspheres	Swelling-osmosis process	PIPS process		
		Sample identity	MMA/SPS weight ratio	Polymerization time of MMA (h)
SPS-R1	Macro-SPS-R1	Macro@Meso-SPS-R1-1	1:5	10
		Macro@Meso-SPS-R1-2	1:2	10
		Macro@Meso-SPS-R1-3	1:1	10
		Macro@Meso-SPS-R1-4	2:1	10
		Macro@Meso-SPS-R1-5	5:1	10
		Macro@Meso-SPS-R1-6	1:1	5
		Macro@Meso-SPS-R1-7	1:1	20
SPS-R2	Macro-SPS-R2	Macro@Meso-SPS-R2	1:1	10
SPS-C	Macro-SPS-C	Macro-SPS-C-P	1:1	10

Table S6 BET surface areas, pore volumes, and the most probable surface pore sizes of different porous microspheres measured by N<sub>2</sub> adsorption-desorption isotherms

Sample identity	BET surface area (m <sup>2</sup> g <sup>-1</sup> )	Pore volume (cm <sup>3</sup> g <sup>-1</sup> )	Most probable surface pore size calculated from BJH method (nm)
Macro@Meso-SPS-R1-1	14.1	0.0431	~ 2
Macro@Meso-SPS-R1-2	15.6	0.0463	11.2
Macro@Meso-SPS-R1-3	5.8	0.0261	44.7
Macro@Meso-SPS-R1-4	12.0	0.0468	45.3
Macro@Meso-SPS-R1-5	5.3	0.0178	> 50
Macro@Meso-SPS-R1-6	14.5	0.0431	14.9
Macro@Meso-SPS-R1-7	16.3	0.1981	> 50
Macro@Meso-SPS-R2	15.0	0.0613	3.1
Macro-SPS-C-P	59.7	0.4217	> 50

## II. Loading and sustained release behaviors of MO from Macro@Meso-SPS microspheres

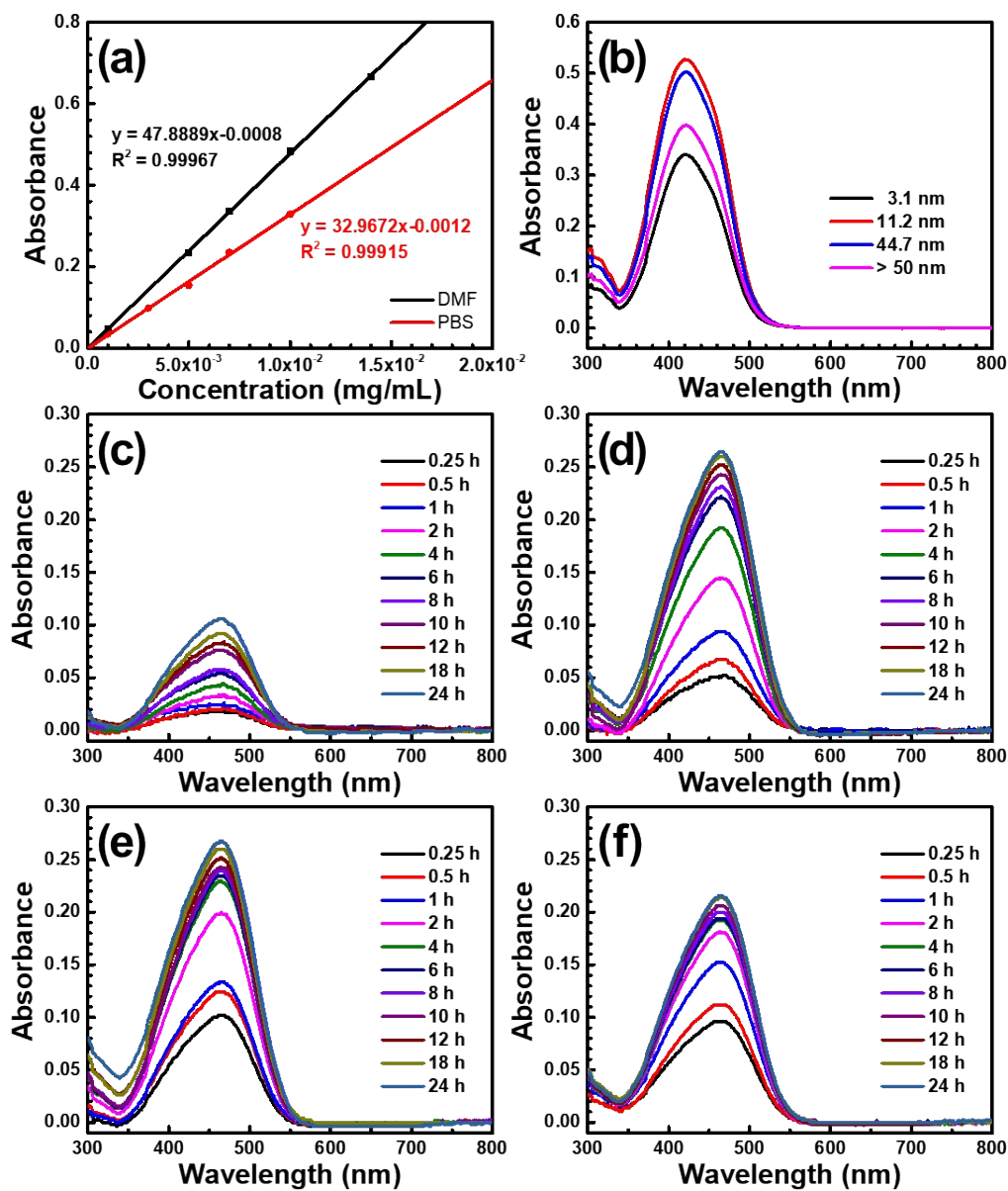


**Fig. S2.** Standard work curves (a) of MO in DMF (black) and PBS buffer (red). UV-vis spectra of different MO-loaded Macro@Meso-SPS microspheres in DMF (b). UV-vis spectra of MO in PBS buffer released from Macro@Meso-SPS microspheres with different surficial pore sizes: 3.1 (c), 11.2 (d), 44.7 (e), and > 50 nm (f).

### III. $^1\text{H}$ NMR spectra of different PS microspheres

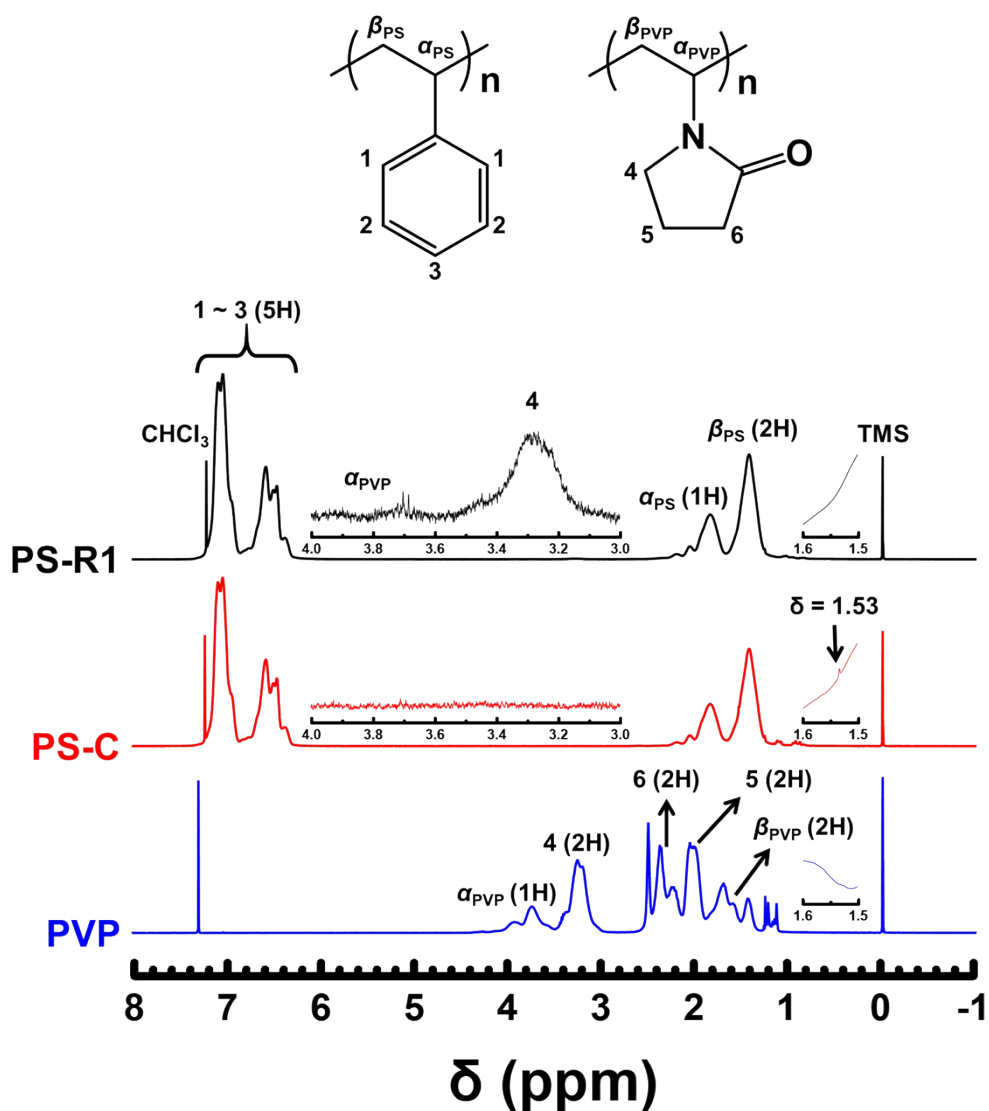


**Fig. S3**  $^1\text{H}$  NMR spectra of PS-R1, PS-C, and PVP in  $\text{CDCl}_3$  (the insets are the corresponding magnified spectra from  $\delta = 1.5 - 1.6$ , and  $3.0 - 4.0$  ppm). The small peak at  $\delta = 1.53$  of PS-C should be attributed to AIBN residues (Fordham, P. J., Gramshaw, J. W., & Castle, L., Food Addit. Contam., 2001, 18, 461.)

#### IV. XPS spectra of PS-R1 and SPS microspheres

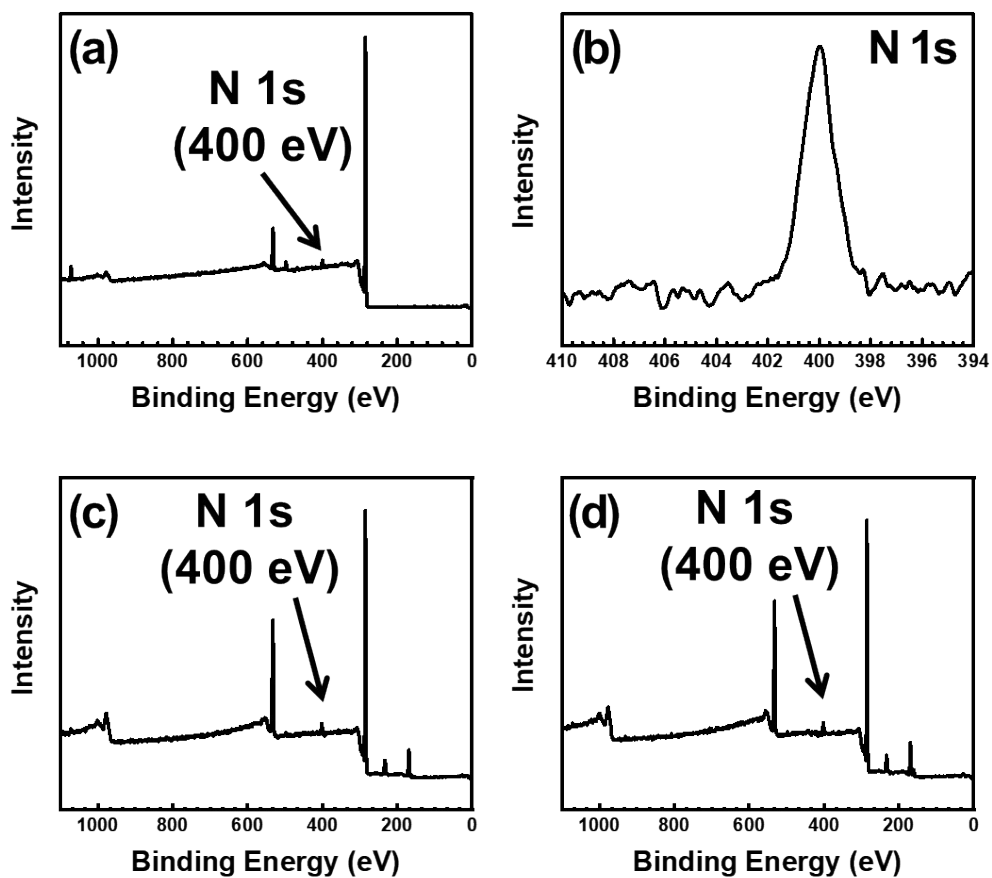


**Fig. S4** Low resolution (a) and N 1s (b) XPS spectra of PS-R1 microspheres; XPS spectra of SPS-R1 (c) and SPS-C (d) microspheres.

## V. Release kinetic models of MO from Macro@Meso-SPS microspheres

The cumulative release ratios ( $R$ ) of MO from hierarchically porous SPS microspheres with different surficial pore sizes (3.1, 11.2, 44.7, and > 50 nm) were fitted by the following three release kinetic models: first-order,<sup>1</sup> Korsmeyer–Peppas,<sup>2</sup> and Higuchi models.<sup>3</sup> Because of burst effect for the highly soluble molecules<sup>4,5</sup> and the rapid release for the residual MO on surface, the above three models are modified as follows:

$$R = (R_e - b_1) \times (1 - e^{-k_1 t}) + b_1 \quad \text{modified first-order model}$$

$$R = k_{KP} \times t^n + b_{KP} \quad \text{modified Korsmeyer–Peppas model}$$

$$R = k_H \times \sqrt{t} + b_H \quad \text{modified Higuchi model}$$

where  $R$  and  $R_e$  are the cumulative release ratios of MO at time  $t$  and at equilibrium.  $k_1$ ,  $k_{KP}$  and  $k_H$  are the release rate coefficients of first-order, Korsmeyer–Peppas and Higuchi kinetic models, respectively.  $n$  is the diffusivity coefficient.  $b_1$ ,  $b_{KP}$ , and  $b_H$  are constants related to the burst effect for the highly soluble molecules and the rapid release of the residual MO on surface. The corresponding kinetic parameters are listed in Table S7.

**Table S7.** The fitting parameters of different kinetic models for the release of MO from different hierarchically porous SPS microspheres

Model	Parameter	Size of surficial pores			
		3.1 nm	11.2 nm	44.7 nm	> 50 nm
First-order	$R^2$	0.992	0.996	0.959	0.945
	$R_e$	$5.35 \times 10^{-1}$	$7.30 \times 10^{-1}$	$7.77 \times 10^{-1}$	$7.91 \times 10^{-1}$
	$k_1$	$7.12 \times 10^{-2}$	$2.75 \times 10^{-1}$	$3.16 \times 10^{-1}$	$5.67 \times 10^{-1}$
	$b_1$	$6.94 \times 10^{-2}$	$1.13 \times 10^{-1}$	$2.79 \times 10^{-1}$	$3.06 \times 10^{-1}$
Korsmeyer–Peppas	$R^2$	0.994	0.865	0.830	0.813
	$k_{KP}$	$7.45 \times 10^{-2}$	$1.59 \times 10^{-1}$	$1.46 \times 10^{-1}$	$2.14 \times 10^{-1}$
	$b_{KP}$	$3.31 \times 10^{-2}$	$1.46 \times 10^{-1}$	$3.00 \times 10^{-1}$	$3.08 \times 10^{-1}$
	$n$	0.551	0.473	0.424	0.305
Higuchi	$R^2$	0.993	0.932	0.904	0.864
	$k_H$	$8.97 \times 10^{-2}$	$1.43 \times 10^{-1}$	$1.08 \times 10^{-1}$	$9.12 \times 10^{-2}$
	$b_H$	$1.74 \times 10^{-2}$	$1.64 \times 10^{-1}$	$3.41 \times 10^{-1}$	$4.38 \times 10^{-1}$

If  $R$  is plotted versus the square root of  $t$ , it is evident that the release curve of Macro@Meso-SPS microspheres with surficial pores around 3.1 nm can fit Higuchi model well (Figure 10B), while the other three porous microspheres also show Higuchi release profiles at the beginning (approximately  $R < 60\%$ ). The fitting results are listed in Table S8.

**Table S8.** The fitting parameters of the release curves for MO from different hierarchically porous SPS microspheres at  $R$  is approximately below 60%.

Parameters	Size of surficial pores			
	3.1 nm	11.2 nm	44.7 nm	> 50 nm
$R^2$	0.993	0.996	0.982	0.991
$k_H$	$8.97 \times 10^{-2}$	$2.50 \times 10^{-1}$	$2.57 \times 10^{-1}$	$3.57 \times 10^{-1}$
$b_H$	$1.74 \times 10^{-2}$	$2.10 \times 10^{-2}$	$1.68 \times 10^{-1}$	$1.74 \times 10^{-1}$

### References

- 1 J. G. Wagner, *J. Pharm. Sci-US*, 1969, **58**, 1253.
- 2 R. W. Korsmeyer, R. Gurny, E. Doelker, P. Buri and N. A. Peppas, *Int. J. Pharmaceut.*, 1983, **15**, 25.
- 3 T. Higuchi, *J. Pharm. Sci-US*, 1963, **52**, 1145.
- 4 W. D. Lindner and B. C. Lippold, *Pharm. Res.*, 1995, **12**, 1781.
- 5 H. Kim and R. Fassihi, *J. Pharm. Sci-US*, 1997, **86**, 323.